Elastic Modulus and Equilibrium Swelling of Poly(dimethylsiloxane) Networks

Suman K. Patel, Shawn Malone, and Claude Cohen*

School of Chemical Engineering, Cornell University, Ithaca, New York 14853-5201

Jeffrey R. Gillmor and Ralph H. Colby

Corporate Research Laboratories, Eastman Kodak Company, Rochester, New York 14650-2110

Received March 20, 1992; Revised Manuscript Received June 25, 1992

ABSTRACT: Model poly(dimethylsiloxane) (PDMS) networks and imperfect networks containing pendant chains and branched structures are prepared by end-linking mixtures of di- and monofunctional PDMS and a tetrafunctional cross-linker. Values of the equilibrium modulus of the networks, obtained from dynamic mechanical experiments, illustrate the importance of the entanglement contribution to the elastic modulus. The extents of equilibrium swelling are determined for the networks in two solvents, toluene and benzene. The predictions from the c^* theorem do not apply to the model networks due to extensive interspersion of the network chains, which leads to entanglements that are not removed by swelling. The Flory–Rehner model, coupled with the phantom network model gives good agreement with swelling results when the experimentally measured elastic modulus is used in the analysis.

Introduction

Several molecular models have been developed which predict the elastic and swelling behavior of polymer networks. Such models are usually developed for model networks, containing no defects. Despite the vast amount of experimental work which has attempted to test and evaluate these models, there is still considerable debate concerning their validity and applicability. Furthermore, for nonperfect networks, little is known about how the structure of a network influences its elastic and equilibrium swelling behavior.

For the affine network model, the shear modulus is given by[1]

$$G_e^{\text{affine}} = \nu RT \tag{1}$$

where ν is the number of moles of elastic chains per unit volume of the network, an elastic chain being a chain attached to the network at each of its two ends. R is the gas constant, and T is the absolute temperature. For the phantom network[2] the junctions (crosslinks) are allowed to fluctuate and the shear modulus is lower than that of an affine network

$$G_e^{\text{phantom}} = (\nu - \mu)RT \tag{2}$$

where μ is the number of moles of junctions per unit volume of the network. Flory and Erman's more recently proposed constrained junction model,[3-5] allows for behavior which is intermediate between the affine and phantom network models:

$$G_e^{\text{phantom}} < G_e^{\text{Flory-Erman}} < G_e^{\text{affine}} \tag{3}$$

The network is predicted to be more affinelike at small deformations and more phantomlike at larger deformations. Contributions to the modulus from points along the contour of the polymer chains are not considered in these models. In the phenomenological model developed by Langley[6] and Dossin and Graessley,[7] an additional term is introduced to allow for a contribution to the modulus from polymer chain entanglements. The result of the model can be expressed as

$$G_e^{\text{Langley-Graessley}} = (\nu - h\mu)RT + G_N^{\circ}\,\text{Te} \tag{4}$$

where h is an empirical parameter between zero and one, G_N° is the plateau modulus of a melt of un-cross-linked, high molecular weight polymer, and Te is the trapping factor, the proportion of the maximum concentration of topological interactions that contribute to the modulus. G_e predicted by this model (eq 4) can be greater than G_e predicted by the affine network model (eq 1). In the more fundamental slip-link model,[8-10] entanglements are modeled as slip-links joining polymer chains together, and may effectively act as additional cross-links. The resulting expression for the modulus is of the same form as eq 4. It allows for intermediate behavior between slip-links acting as chemical cross-links and slip-links being elastically ineffective. Both the Langley–Graessley model and the slip-link model allow the predicted modulus to exceed the affine network modulus (eq 1) and hence exceed any prediction of the Flory–Erman model (eq 3).

The extent of swelling that networks undergo when placed in a good solvent is predicted by various models. The Flory–Rehner expression for the swelling of a polymer network[1,11] based on the assumption of additivity of the free energy of mixing and the free energy of elasticity leads to

$$\ln(1 - v_2) + v_2 + \chi v_2^2 = \mathrm{v}_1\nu\left[\frac{v_2}{2} - v_2^{1/3}\right] \tag{5}$$

for the tetrafunctional affine network model and

$$\ln(1 - v_2) + v_2 + \chi v_2^2 = -\mathrm{v}_1(\nu - \mu)v_2^{1/3} \tag{6}$$

for the phantom network model, where v_2 is the polymer volume fraction at equilibrium swelling, χ is the polymer–solvent interaction parameter, and v_1 is the molar volume of solvent. For an ideal perfect network prepared by end-linking, ν should be the number density of precursor chains that was used to prepare the network, since it is assumed that every precursor molecule becomes an elastic chain. However, in real networks, nonidealities, which are always present, such as the presence of pendant chains (which are linked to the network at only one end), will decrease ν, whereas the nonideality of entrapped entanglements will increase ν, since the number of "effective cross-links"

0024-9297/92/2225-5241$03.00/0

(due to entrapped entanglements) is increased.[12,13] The c^* theorem proposed by de Gennes[14] makes an analogy between semidilute polymer solutions and equilibrium swollen polymer networks. It postulates that the swollen network will achieve an equilibrium concentration, which is proportional to the overlap concentration in semidilute solutions, c^*:

$$v_2\rho_2 \sim c^* \tag{7}$$

where ρ_2 is the polymer density. By scaling arguments, de Gennes[14] shows that $c^* \sim M^{-4/5}$ where M is the molecular weight of the chains, therefore

$$v_2\rho_2 \sim M^{-4/5} \tag{8}$$

There is still considerable debate and ongoing research concerning the validity and applicability of the models discussed above. Some argue that entanglements or interchain interactions only affect the elastic and swelling properties of the networks by restricting the fluctuations of the cross-links.[15-19] Others have argued that the entanglements between polymer chains can act similarly, although perhaps not as effectively, as actual chemical cross-links.[20-26] These workers argue that the number of cross-links in a network must be modified to include an entanglement contribution and that only models that possess entanglement contributions to the modulus, such as the model developed by Langley and Graessley[6,7] or Edward's slip-link model,[8,10] can successfully predict polymer network behavior. Furthermore, the validity of the Flory–Rehner assumption of additivity of free energies, the basis of all of the swelling models discussed above, has also been called into question by the work of a few groups[27,28] and aside from the dependence of χ on v_2, its potential dependence on the extent of cross-linking (ν) has also been raised.[29]

One of the earliest studies of the effect of pendant chains on the physical properties of polymer networks was performed on polystyrene–divinylbenzene (PS–DVB) networks prepared by an anionic block copolymerization technique.[30] The workers found that although the compression modulus decreased markedly as the number of pendant chains was increased, the extent of network equilibrium swelling in benzene hardly changed at all. However, it was later found that the networks are composed of DVB nodules or clusters, from which many polystyrene chains emanate.[31] The average functionality of these networks is thus unknown and the cross-link functionality can vary considerably from nodule to nodule. Intuitively, introducing pendant chains should have a less pronounced effect upon the equilibrium swelling of high-functionality networks, which may explain the small change in equilibrium swelling with increasing pendant chain concentration in the polystyrene–DVB networks.

A later study was performed on end-linked poly(dimethylsiloxane) (PDMS) networks, prepared with bifunctional PDMS and a tetrafunctional cross-linker.[32] The pendant chains were introduced into the networks by using an excess of the bifunctional polymer. Although these workers wrote that the effect of pendant chains on equilibrium swelling was a relatively small effect, they found that v_2 decreased from ~0.315 to 0.204 (quite appreciable) when the percentage of dangling ends increased from 4.7 to 41.7%. This study was performed on networks that were better characterized than the polystyrene/divinylbenzene networks and indicated an appreciable effect on swelling.

Table I
Molecular Weights of PDMS Precursors

sample	M_n	M_w/M_n
	Difunctional Precursors	
1	2 460	1.15
2	6 160	1.17
3	8 350	1.25
4	10 900	1.19
5	16 800	1.20
6	18 500	1.18
7	19 800	1.24
8	20 100	1.21
9	28 200	1.23
10	53 500	1.27
11	58 000	1.25
	Monofunctional Precursors	
12	19 800	1.26
13	71 200	1.70

We report here results on two types of polymer networks with widely varied and reasonably well-controlled structures. The first type is denoted as model networks and was prepared by end-linking pure difunctional PDMS (B_2). The second type is denoted as imperfect networks and was prepared by end-linking mixtures of B_2 and monofunctional PDMS (B_1). The types of structures obtained in these networks can be modeled and thus provide a great advantage over conventional methods of network synthesis. Dynamic mechanical experiments on the dry networks and equilibrium swelling measurements in toluene and in benzene were performed in order to examine the theoretical models.

Experimental Section

Materials. The B_2 precursor chains were prepared by polymerizing hexamethylcyclotrisiloxane (D_3) in toluene, using methyl sulfoxide as a promoter, and benzyltrimethylammonium bis(*o*-phenylenedioxy)phenylsiliconate as a catalyst.[33-35] B_2 was encapped with vinyl groups using vinyldimethylchlorosilane and pyridine as an acid scavenger; it was washed with water, dissolved and reprecipitated with toluene and methanol, and then dried in a vacuum oven at 60 °C for 3 days.

B_1 was synthesized by polymerizing D_3 in cyclohexane, using *n*-BuLi as an initiator and methyl sulfoxide as a promoter. B_1 was endcapped, washed, and dried using the same methods as were used in the preparation of B_2.

B_2 and B_1 were characterized using gel permeation chromatography and the Mark–Houwink parameters obtained by Lapp et al.[36] The results are reported in Table I.

Experimental Methods. The networks were synthesized using methods which have been well established.[26,37,38] The networks were formed using a hydrosilation reaction: a platinum-catalyzed addition of silane hydrogens, present on the cross-linker molecule, tetrakis(dimethylsiloxy)silane (A_4), to the vinyl groups at the ends of the polymer molecules. B_2, B_1, and A_4 were mixed and stirred and the reaction was catalyzed with *cis*-dichlorobis(diethyl sulfide)platinum(II) in toluene to achieve a concentration of 20 parts platinum/10^6 parts PDMS. For the elastic property measurements, the mixture was poured directly onto the lower plate of the rheometer immediately after the catalyst was added. The samples were then allowed to cure between the parallel plates overnight in an inert (N_2) atmosphere at a temperature of 30 °C. The moduli measurements were performed on the following day. For samples with $M > 35\,000$, the overnight cure was not sufficient for complete reaction and these samples were cured for 3 days.

Storage and Loss moduli (G' and G'') were obtained in oscillatory shear using a Rheometrics System Four mechanical spectrometer with the parallel plate geometry. The plates were 25 mm in diameter, and the gap between the plates ranged from approximately 1.0 to 1.5 mm. After the samples were analyzed (at 30 °C), they were removed from the rheometer and w_{sol}, the

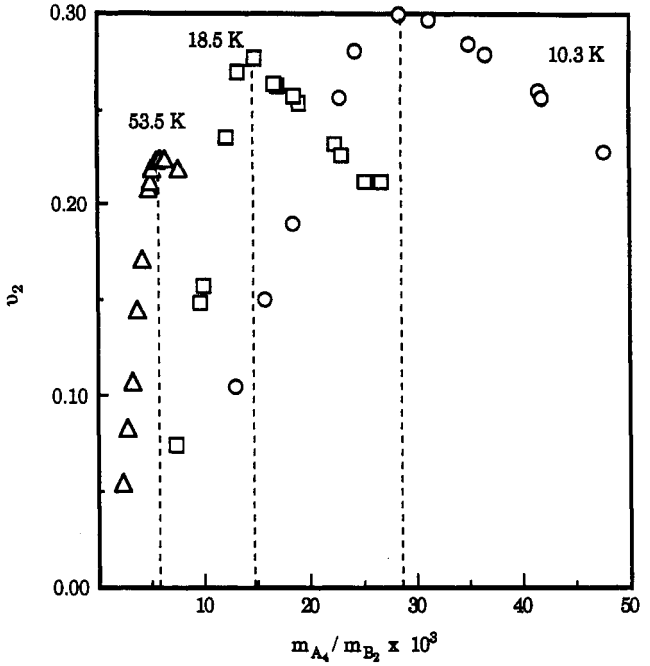

Figure 1. Typical plots used to determine the optimum weight ratio of A_4 to B_2. The labels 53.5 K, 18.5 K, and 10.3 K represent B_2 molecular weights of 53 500, 18 500, and 10 300, respectively.

weight fraction of soluble material, and v_2 in toluene and benzene were determined using standard procedures.[39]

The Macosko and Miller model[40-42] of nonlinear polymerization was used to calculate ν, μ, and $M_{n,el}$, the number average molecular weight of the elastic chains (excluding any attached pendant chains), for each of the networks. The expressions which result from the application of this model to the case of the copolymerization of A_4 with B_1 and B_2 are given in the Appendix. $M_{n,el}$ (from eq A7), ν (from eq A9), and μ (from eq A10) depend upon the relative amounts of the initial reactants and on the extent of reaction, p. The relative amounts of the reactants are easily calculated from the masses of A_4, B_2, and B_1 used to prepare the networks. The extent of reaction was determined from the experimental values of the soluble fraction, as has been suggested by Valles and Macosko.[20]

Results and Discussion

Elastic Behavior. Both model and imperfect networks were prepared. The model networks were prepared using B_2 with molecular weights ranging from 2.5K to 58K. The amount of cross-linker (A_4) used to prepare each network was that which gave the networks with the lowest degree of equilibrium swelling (the maximum value of v_2). For each B_2, networks with various weight ratios of A_4 to B_2 were prepared, and the optimum amount of A_4 was taken as that which gave a maximum value of v_2, as shown in Figure 1. The number average molecular weights of the precursors used to prepare the networks are given in Table II along with the experimental values of the weight fraction of the soluble material, w_{sol}, and v_2 in toluene.

The optimum amounts of A_4 obtained from plots such as those shown in Figure 1 correspond to values of r (the ratio of silane hydrogens to vinyl groups), r_{opt}, which have been used in the preparation of our networks and are appreciably greater than unity (see Table II). The large values of r used in the preparation of our networks raise the concern of a possible side reaction involving silane hydrogens and backbone Si–O bonds. Such a side reaction would consume silane hydrogens and would use up all cross-linkers beyond the stoichiometric ratio, $r = 1$. Although observed at elevated temperatures,[43] such a side reaction has been shown to be negligible when the networks are cured around room temperature.[44,45] Furthermore,

Table II
Experimental Characteristics of Model Networks

sample designation	$10^{-3}M_{n,B_2}$	r	$10^2 w_{sol}$	v_2	G_e/RT (mol/m³)	$\frac{G_e/RT}{(1-w_{sol})^{1/3}}$ (mol/m³)
A-1	2.46	1.44	0.374	0.442	303	303
A-2	6.16	1.51	0.281	0.354	184	184
A-3a	8.35	1.72	0.450	0.317	149	149
A-3b	8.35	1.61	0.436	0.326	154	154
A-4	10.3	1.82	0.353	0.312	156	156
A-5	10.9	1.46	0.556	0.317	149	149
A-6	16.8	1.53	2.78	0.238	74.2	74.9
A-7a	18.5	1.69	0.259	0.287	130	130
A-7b	18.5	1.69	1.21	0.264	102	102
A-8a	19.8	2.05	0.254	0.276	107	107
A-8b	19.8	2.05	0.573	0.275	109	109
A-9	20.1	1.71	1.14	0.260	82.2	82.5
A-10	28.2	1.68	0.550	0.257	82.2	82.3
A-11	53.5	1.95	0.236	0.246	79.4	79.4
A-12	58.0	1.61	2.63	0.217	74.2	74.9

the existence of r_{opt}, the presence of a fairly sharp maximum in Figure 1, does not support an attack on the backbone by silane hydrogens, as such a reaction would lead to progressively tighter networks as r is increased. The only side reaction that is known to occur at 30 °C is a cross-linker redistribution,[46] which leads to a higher functionality cross-linker and should not affect our results. There are two explanations for why $r_{opt} > 1$. First, steric hindrance will probably result in an unequal reactivity of the reactive sites of a given A_4 molecule. That is, the reactivity of a silane hydrogen will depend upon how many of the other three sites of the A_4 molecule to which it is attached have already reacted. The case of unequal reactivity in vinyl copolymerization, for example, is well documented.[47,48] Second, titration, proton NMR, and preliminary gas chromatography/mass spectrometry on our precursor polymers indicate that there are more vinyl groups than one per chain end. From the GC/mass spectrometry results which are sensitive only to very low molecular weight species, the additional vinyl groups appear to be present in low molecular weight species. These species would also lead to higher functionality cross-linkers and should not affect our results.

Two series of imperfect networks were prepared. In the first, we used a B_2 with $M_n = 20\,100$ and a B_1 with $M_n = 19\,800$ (samples 8 and 12 of Table I). For the second series of imperfect networks, we used a B_2 with $M_n = 58\,000$ and a B_1 with $M_n = 71\,200$ (samples 11 and 13 of Table I). The molar fraction of monofunctional precursors, x, ranged from zero to 60%. The value of r in these networks was kept approximately constant, equal to the optimum value of r determined for the preparation of a model network from the same B_2 used in the preparation of each series of networks. The characteristics of the individual imperfect networks are given in Table III. Also given in Table III are the experimental values of w_{sol} and v_2 in toluene.

A typical plot of G' and G'' versus frequency, ω, for a model network is given in Figure 2a. The values of G' are observed to be several orders of magnitude greater than those of G'' for frequencies ranging from 10^{-3} to 100 rad/s. The noise in G'' at low frequencies is due to the usual difficulties in precision for determining a phase angle close to zero. The fact that the phase angle is so close to zero ($G' \gg G''$) indicates that these model networks contain only a small amount of imperfections. Because the networks were cured in situ, the variations of G'' in the range 10–100 rad/s are due to the soluble fraction and pendant chains. The soluble fraction was analyzed by

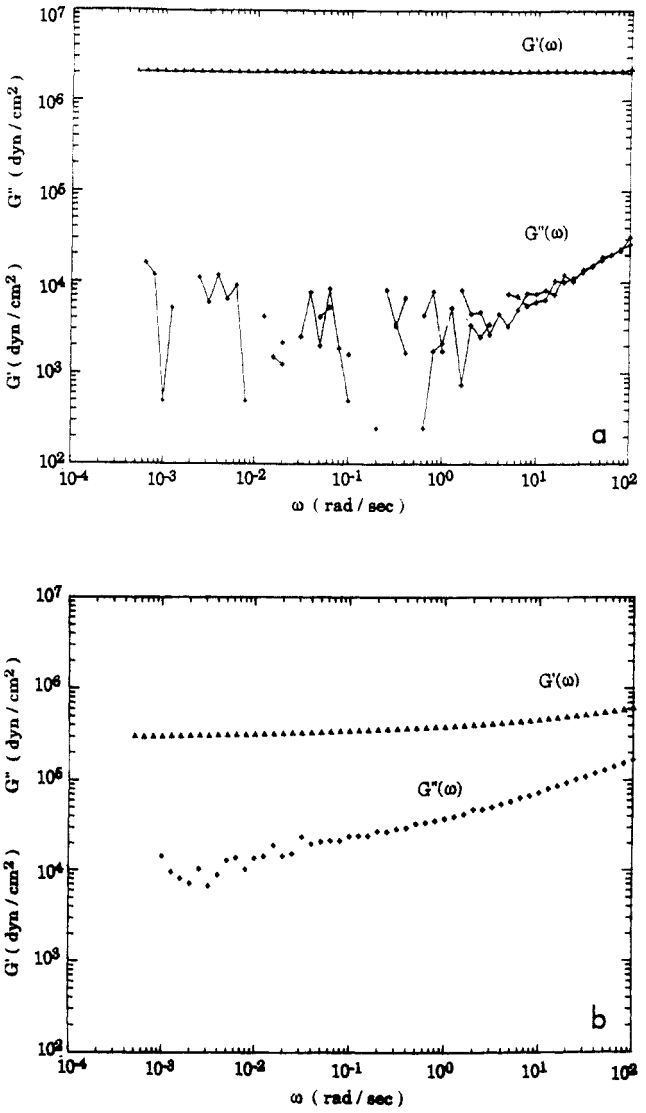

Figure 2. (a) Storage and loss modulus data for model network A-9. (b) Storage and loss modulus data for imperfect network B′-4.

Table III
Experimental Characteristics of Imperfect Networks

network	x	r	$10^2 w_{sol}$	ν_2	G_e/RT (mol/m³)	$G_e/RT(1-w_{sol})^{1/3}$ (mol/m³)
		M_{n,B_2} = 20 100, M_{n,B_1} = 19 800				
B-1	0.0	1.64	1.14	0.260	82.2	82.5
B-2	0.051	1.64	2.52	0.238	66.2	66.7
B-3	0.146	1.65	4.36	0.227	57.3	58.2
B-4	0.296	1.64	7.74	0.200	36.0	36.9
B-5	0.445	1.65	11.8	0.170	29.0	30.2
B-6	0.596	1.65	18.9	0.130	17.0	18.2
		M_{n,B_2} = 58 000, M_{n,B_1} = 71 200				
B′-1	0.0	1.61	2.63	0.217	74.2	74.9
B′-2	0.170	1.47	6.98	0.183	35.6	36.5
B′-3	0.336	1.49	14.5	0.143	21.8	23.0
B′-4	0.482	1.44	27.8	0.094	11.8	13.2
B′-5	0.622	1.42	39.6	0.066	4.45	5.26

GPC to show that it consisted primarily of precursor chains and a wide distribution of higher molecular weights. Since the values of G' appear to be constant over a very broad range of frequencies, this constant value of G' can be taken as equal to G_e, the equilibrium modulus of the network. Similar results were observed for the first series of imperfect networks, and it is only in the second series of imperfect networks at high values of x (i.e., high mole fraction of B_1 precursors) that relaxation in G' could clearly be observed, as shown in Figure 2b. However, in the experiments performed here, the soluble fraction of the network has not been removed and acts as a diluent. The soluble fraction and pendant branched structures of the network are relaxing during the measurement of the elastic modulus. Analysis of this relaxation may therefore be complex and will not concern us here. In this case, G_e is taken as the asymptotic value of G' at low frequency. To calculate the modulus of the dry network after extraction, we calculate the volume fraction u_2 of polymer in the network as

$$u_2 = 1 - u_{sol} = 1 - w_{sol} \tag{9}$$

where the last equality in eq 9 follows from the fact that the density of the soluble fraction is equal to the density of the network chains. We then use a correction derived by Flory[1] for a network swollen in a solvent. For the affine network model this gives

$$G_e/RT = \nu(1 - w_{sol})^{1/3} \tag{10}$$

As seen in Tables II and III, this correction is extremely small for the model networks (<1%) and is still quite small for the imperfect networks (<20%). We ignore this correction in this paper, as its incorporation does not lead to any appreciable change of the results.[49]

The moles of elastic chains per unit volume of dry network after extraction, ν, must be determined in order to compare the experimental values of G_e with the theoretical models. For the model networks, the soluble fractions reported in Table II are quite low, and to a first approximation, the molecular weight of the elastic chains have often been taken as M_{n,B_2}, the molecular weight of the B_2 precursors used to prepare the network. Then, ν can be expressed as $\rho_2/M_{n,B_2}$ where ρ_2 is the density of the polymer taken to be 0.9697 g/cm³ for PDMS. However, this appears to be a poor approximation even for model networks with small soluble fractions, as will be shown later. Therefore, the Macosko–Miller[40-42] model of nonlinear polymerization was used to evaluate ν for both the perfect and imperfect networks. This model also provides expressions for $M_{n,el}$ and μ. The resulting values of $M_{n,el}$, ν, and $(\nu - \mu)$ are reported in Tables IV and V for model networks and imperfect networks, respectively. Comparing the second and fourth columns in Table IV, it is apparent that the values of ν calculated assuming $\nu = \rho_2/M_{n,B_2}$ are significantly greater than the values of ν calculated using the Macosko–Miller model. This is due to the fact that even networks with very low soluble fractions, such as the model networks prepared, have an

Table IV
Model Network Characteristics Based upon the Macosko–Miller Model

sample designation	$\rho_2/M_{n,B_2}$ (mol/m³)	$10^{-3}(M_{n,el})$	ν (mol/m³)	$\nu - \mu$ (mol/m³)	μ/ν
A-1	394	3.48	242	96.2	0.602
A-2	157	8.64	100	39.6	0.604
A-3a	116	13.1	64.5	24.7	0.617
A-3b	116	12.5	67.7	26.2	0.613
A-4	93.8	17.1	50.9	19.3	0.620
A-5	88.8	19.2	43.8	16.4	0.625
A-6	57.5	28.8	24.0	9.03	0.623
A-7a	52.5	27.9	31.5	12.2	0.614
A-7b	52.5	31.1	24.9	9.41	0.622
A-8a	49.1	34.2	26.0	9.76	0.624
A-8b	49.1	36.6	22.9	8.53	0.628
A-9	48.3	32.5	24.0	9.14	0.619
A-10	34.4	41.9	19.9	7.71	0.613
A-11	18.1	85.2	10.3	3.95	0.618
A-12	16.7	102	6.87	2.58	0.624

Table V
Imperfect Network Characteristics Based upon the Macosko–Miller Model

sample designation	$10^{-3}M_{n,el}$	ν (mol/m^3)	$\nu - \mu$ (mol/m^3)	μ/ν
	M_{n,B_2} = 20 100, M_{n,B_1} = 19 800			
B-1	32.5	24.0	9.14	0.619
B-2	35.1	19.9	7.47	0.625
B-3	37.9	16.2	6.02	0.629
B-4	42.9	11.5	4.21	0.634
B-5	50.0	7.65	2.75	0.640
B-6	63.9	4.08	1.44	0.647
	M_{n,B_2} = 58 000, M_{n,B_1} = 71 200			
B′-1	102	6.87	2.58	0.624
B′-2	109	4.94	1.84	0.629
B′-3	137	2.75	0.995	0.638
B′-4	190	1.23	0.436	0.647
B′-5	261	0.553	0.192	0.653

average effective degree of functionality less than 4 and a certain amount of pendant chains. These latter defects reduce the number of elastic chains, causing ν calculated from the Macosko–Miller model to be lower than $\rho_2/M_{n,B_2}$. The ratio μ/ν should equal $^1/_2$ for ideally perfect tetrafunctional networks and $^2/_3$ for ideally perfect trifunctional networks. The results in the last column of Table IV indicate that our "model" networks have an average functionality around 3.2 based on a Macosko–Miller calculation, which is quite short of the value of 4 expected for a defect-free model network. We note that, for the imperfect networks listed in Table V, we find, as expected, that the average functionality decreases (i.e. μ/ν increases) as the networks become more imperfect.

In Figure 3, the experimental values of G_e/RT reported in Table II for the model networks are plotted versus the calculated Macosko–Miller values of ν reported in Table IV. Figure 3 directly tests the affine network model (eq 1). One should note that the soluble fraction correction of eq 10 would only raise the data further above the affine prediction (solid line). Clearly, the affine network model and, hence, the Flory–Erman model (eq 3) fail for the data of Figure 3. The modulus is grossly underpredicted by the affine network model, particularly for the networks made from long precursor chains (lowest ν), where the underprediction exceeds a factor of 10! This is strong evidence that some other source of elasticity must be important (trapped entanglements, eq 4). In fact, the data of Figure 3 are reasonably consistent with eq 4 with h = 0 and Te = 1 (a simple vertical shift of the affine prediction). This is the simplest possible idea about entanglements—the cross-links deform affinely and the extra contribution to the modulus due to entanglement is simply the plateau modulus of the un-cross-linked melt.[7,20]

$$G_e = \nu RT + G_N^\circ \qquad (11)$$

The results have some of the same qualitative trends as the results reported by Opperman and Rennar,[23] who conducted uniaxial deformation experiments on PDMS networks. Because these workers use $\nu = \rho/M_{n,B_2}$ and do not report values of r and w_{sol} in the preparation of their networks, a direct comparison cannot be made. They observed three regimes: (i) for small values of ν, the values of G_e decreased sharply with decreasing ν; (ii) for networks with intermediate ν values, G_e remained relatively constant and independent of ν; (iii) for networks with high ν, G_e increased proportionally with ν.

The sharp decrease in G_e with decreasing ν for small values of ν observed by Opperman and Rennar[23] is not reproduced in our results. In fact, the results reported in Figure 3 for the model networks do not give any indication

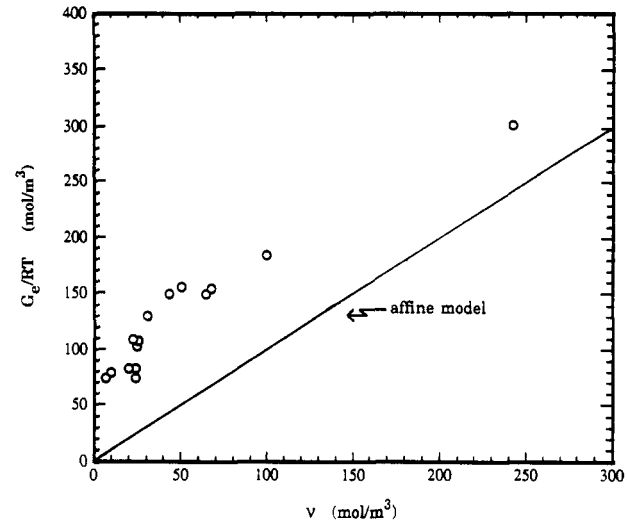

Figure 3. Equilibrium shear moduli of model networks plotted as G_e/RT versus ν calculated from the Macosko–Miller model. The straight line represents the behavior predicted by the affine network model.

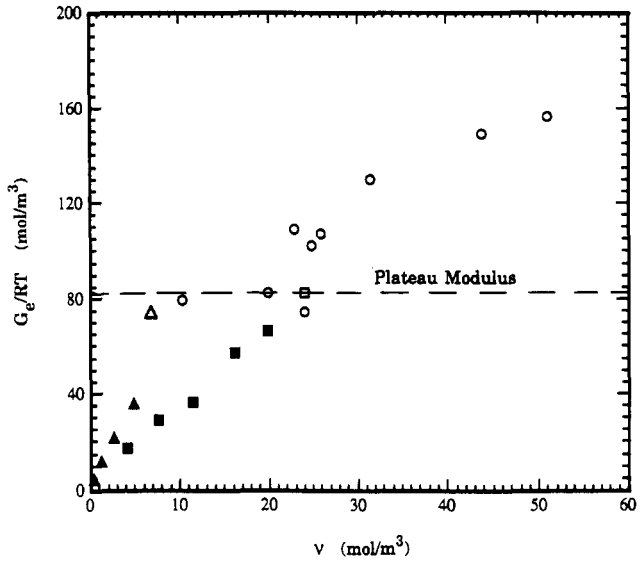

Figure 4. Equilibrium shear moduli of all of the networks with low ν plotted as G_e/RT versus ν calculated from the Macosko–Miller model. The open symbols are for the model networks. The symbols ■ and ▲ are the data for the B and B′ imperfect network series, respectively, from Table V. The dashed line is the average value of previously reported plateau moduli from ref 20 and 50.

of a significant decrease in G_e/RT at small ν from a plateau value, as can be seen more clearly in Figure 4. The value of G_e in the constant modulus regime was observed to be slightly lower than the value observed by Opperman and Rennar[23] in their intermediate ν regime. However, considering the experimental uncertainty in our values and in theirs, the resulting values of G_e in the constant modulus regime are essentially the same and are very close to the plateau modulus of high molecular weight, un-cross-linked PDMS, which has been reported by Plazek et al.[50] and Valles and Macosko[20] to be 2.0 and 2.11 × 10^6 dyn/cm^2, corresponding to values of G_e/RT of 79 and 84 mol/m^3, respectively. These results indicate that the modulus of model networks with precursor B_2 chains above a certain molecular weight ($M_{n,B_2} \simeq$ 20K) is dominated by trapped entanglements and not chemical cross-links. It is interesting to note that above a molecular weight of linear PDMS of about 20K one expects a rubbery plateau modulus.[51]

No explanation was offered by Opperman and Rennar for the sharp decrease in G_e for their networks with low ν. From the results reported here and from further evidence to come below from our imperfect network series, this previously observed sharp decrease may be caused by network imperfections. The plateau region for our work continued to the lowest value of ν examined ($\nu \simeq 6$ mol/m^3), and the sharp drop in G_e previously reported may be due to the difficulty of obtaining good, defect-free networks from high molecular weight precursors. These results might also be explained if the networks exhibiting these very low values of G_e have been prepared with a stoichiometric value of r ($r \approx 1$) rather than the optimum r used here. Both the results reported here and those reported by Opperman and Rennar indicate, however, that interchain entanglements make an appreciable contribution to the elastic modulus of the networks, giving values for the modulus appreciably higher than the Flory–Erman model and the affine network model. We note that if we had used $\nu = \rho_2/M_{n,B_2}$ in place of the calculated value of ν according to Macosko and Miller, our data would fall on a line with a slope less than unity, but with an intercept still much higher than zero.

The experimental results of the modulus versus the calculated ν values for the two series of imperfect networks are shown in Figure 4 as filled data points. These data indicate a markedly different behavior from that of the model networks. The imperfect networks exhibit values of G_e/RT which quickly drop from the plateau value in almost a linear fashion as ν decreases and the networks become more imperfect. Assuming that the modulus is proportional to ν for these networks, the proportionality constant is higher for series B′ (with B_2 = 58K) than for series B (with B_2 = 20K), and it is much higher than unity (expected for the affine model) for both series.

An explanation of this behavior is that the progressive addition of pendant chains to a network, due to additional quantities of B_1, decreases the effect of the entanglement contribution to the modulus by releasing trapped entanglements that act as effective cross-links. Either the addition of more B_1 to an imperfect network or the increase in the molecular weight of the B_2 precursors in a model network results in a decrease in the values of ν. However, for a given value of ν, the former process leads to a network with shorter elastic chains and more pendant chains than the latter process does. This is easily seen by considering two networks with equal values of ν, one (model network) with no significant amount of pendant chains and the other with a large amount of pendant material. In order for both of the networks to have the same value of ν, the average size of the elastic chains must be lower in the imperfect networks than in the former. Since shorter elastic chains have fewer entanglements than longer elastic chains, the addition of B_1 releases appreciably more trapped entanglements in series B′ than in series B leading to the faster drop of the modulus with ν, observed experimentally.

Equilibrium Swelling Behavior. We have shown that the affine model underpredicts the modulus of the prepared PDMS networks if the role of interspersion and trapped entanglements is not taken into account. We therefore expect the Flory–Rehner model, based on any of the simple models of elasticity that ignore trapped entanglements (e.g. eq 5 or eq 6) to fail. This is shown for the swelling results of our model networks in toluene in Figure 5a,b for the affine and phantom network models, respectively. Figure 5a is plotted assuming a tetrafunctional network and the factor of $^1/_2$ in the denominator of

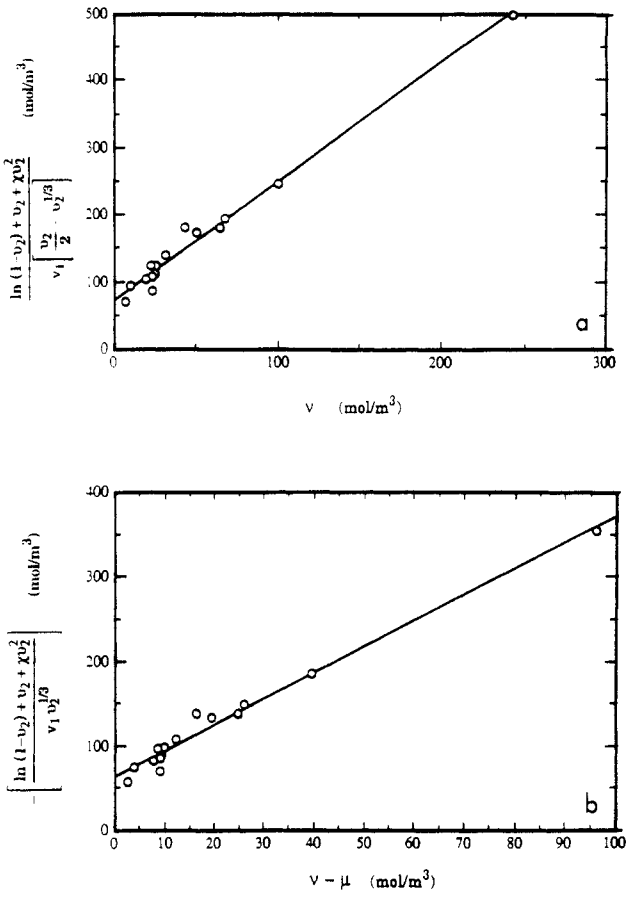

Figure 5. (a) Swelling results from model networks in toluene analyzed in terms of the Flory–Rehner model with the affine network assumption where ν is calculated from the Macosko–Miller model. (b) Same as in (a) but for the phantom network where $\nu - \mu$ is again calculated from the Macosko–Miller model. Lines are least-squares regression fits to the data.

the ordinate should be replaced with μ/ν for networks with functionality different from 4. However, because the use of the calculated values of μ/ν reported in Tables IV and V instead of $^1/_2$ results only in a minor change (about 5%) in the slopes of the various experimental data and will make the ordinate dependent on the branching model, the factor of $^1/_2$ was kept in Figures 5a and 6a. The value of $\chi = 0.445 + 0.297v_2$ obtained from the literature[52] on linear PDMS chains in toluene was used in the ordinate as well as a value of v_1 = 106.9 cm^3/mol. The slopes of the best-fit lines in Figure 5a,b are 1.78 and 3.08, respectively, and the intercepts of these lines are nonzero, clearly violating the predictions of the models (the slopes should be unity and the intercepts should be zero).

The swelling results from the imperfect networks, shown in Figure 6a,b, are markedly different from those of the corresponding model networks, indicated by the dashed lines. Each series of imperfect networks has its own ν dependence, falling to approximately zero with decreasing ν (or $\nu - \mu$). The dependence of swelling on ν (or $\nu - \mu$) for these networks is much stronger than for the model networks. In Figure 6, the slopes of the best fit line through the swelling results of the B′ networks (triangles) are 9.8 for the affine model and 20.9 for the phantom model. These observations are consistent with the elastic behavior discussed in the previous section (see Figure 4). The model networks are more effective at trapping entanglements as compared to the imperfect networks. That is, a network with many pendant chains is expected to be less effective at permanently trapping entanglements than a network with an equivalent value of ν but with few pendant chains.

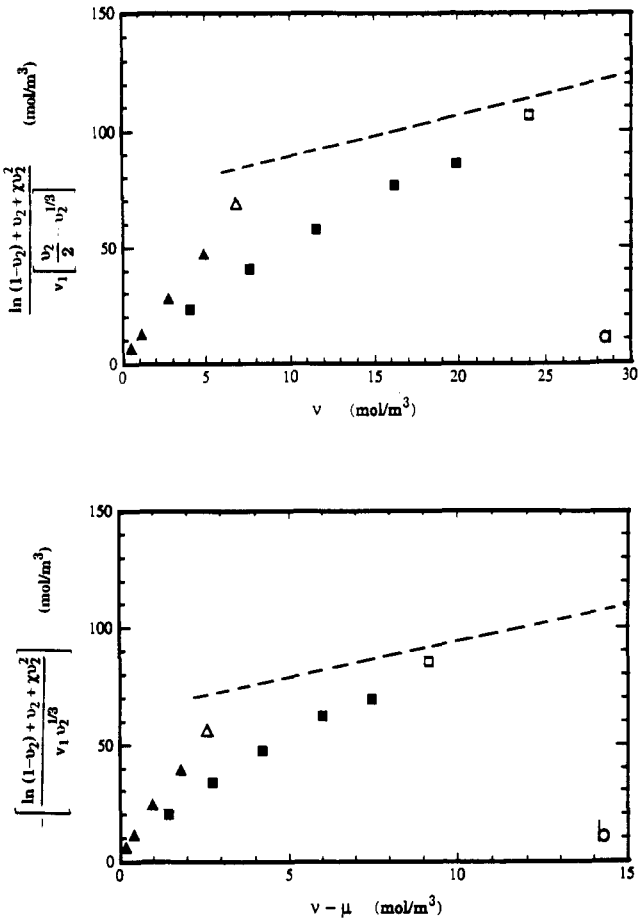

Figure 6. (a) Swelling results from imperfect networks in toluene analyzed in terms of the Flory–Rehner model with the affine network assumption. (b) Same as in (a) but with the phantom network assumption. The dashed lines are the best fit lines of Figure 5. The symbols are the same as in Figure 4.

We have shown[49,53] that the swelling results from imperfect networks made with the same difunctional B_2 chains and monofunctional B_1 chains of different molecular weights were insensitive to the molecular weight of B_1, giving a single v_2 versus ν curve and indicating that the freeing up of trapped entanglements by the addition of B_1 is not strongly influenced by the molecular weight of B_1.

The results reported above are in contrast with the reports of previous workers on PDMS networks swollen in benzene and toluene, which indicated reasonable agreement with the Flory–Erman model.[18,19] That is, when plots such as that given in Figure 5a are constructed for these networks, slopes that are less than unity are obtained. The ordinate in Figure 5a can be interpreted as the Flory–Rehner prediction for the density of elastic chains. It should be noted that in the earlier studies, the soluble fractions of the model networks were higher than in our model networks; on the order of 1.2–6.0%[18] and 3–4%,[19] as compared to less than 1% (with a few exceptions) in this work. The higher soluble fractions in the networks used in the previous studies indicate that these networks contain more network defects and the relation $\nu = \rho_2/M_{n,B_2}$ for perfect model networks used in these works cannot be assumed. Use of $\rho_2/M_{n,B_2}$ instead of ν for our data in Figure 5a would still lead to the same discrepancy that the measured number of elastic chains in the networks, obtained from the Flory–Rehner affine swelling expression (ordinate in Figure 5a), is greater than the calculated number of elastic chains. We note that some workers[20] have obtained swelling results in agreement with the results reported here.

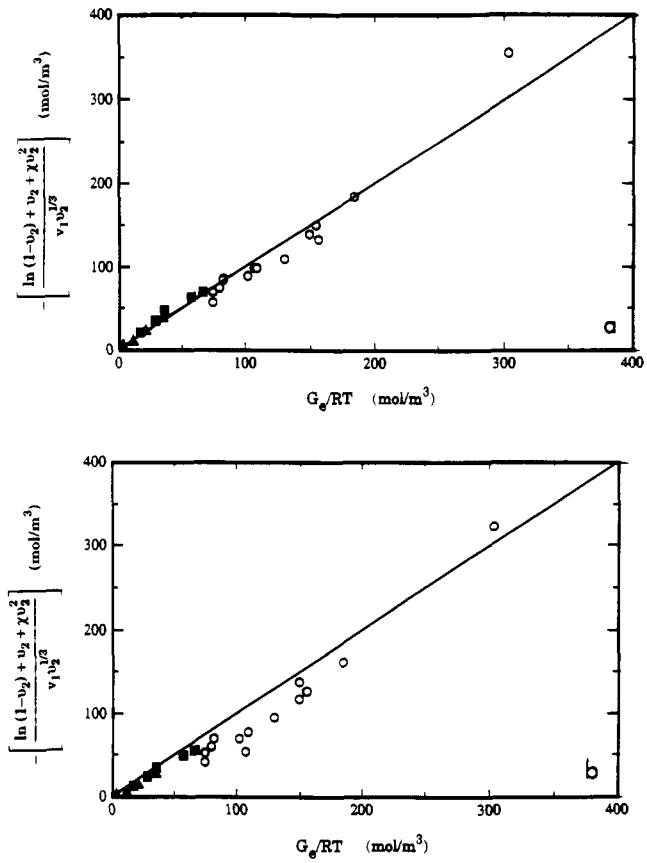

Figure 7. (a) Comparison of the swelling results from all the networks in toluene with the Flory–Rehner prediction assuming the phantom network model applies and using the experimentally determined value of the modulus. (b) Same as in (a) but for benzene. The symbols are the same as in Figure 4.

The number of entanglements and their effectiveness at creating elastic strands are difficult to quantify, even though the slip-link model of Edwards and his collaborators appears to be reasonably successful in describing the mechanical properties of networks.[54] Here, we are interested in the relation between mechanical properties and equilibrium swelling and the validity of the Flory–Rehner assumption. To pursue this with our networks without having to rely on a model to determine ν_{eff}, the total number of effective elastic strands, we replace νRT and $(\nu - \mu)RT$ in eqs 5 and 6 by the experimentally determined modulus and obtain (see eqs 1 and 2)

$$\frac{\ln(1-v_2) + v_2 + \chi v_2^2}{V_1\left[\frac{v_2}{2} - v_2^{1/3}\right]} = \frac{G_e}{RT} \tag{12}$$

$$-\left[\frac{\ln(1-v_2) + v_2 + \chi v_2^2}{V_1 v_2^{1/3}}\right] = \frac{G_e}{RT} \tag{13}$$

where G_e is the equilibrium modulus of the unswollen network. G_e/RT has replaced the unknown factors of ν (for the tetrafunctional affine network) and $\nu - \mu$ (for the phantom network), thereby including any effect of trapped entanglements on swelling. Therefore, eqs 12 and 13 are direct predictions of the original postulate of Flory and Rehner, that swelling is determined by a balance between osmotic and elastic forces.

Equation 13 is tested in Figure 7a,b for both the model and imperfect networks in each solvent. The interaction parameter for PDMS–benzene used in these calculations is that reported by Flory and Shih:[55] $\chi = 0.484 + 0.33v_2$ and V_1 for benzene is taken as 89.41 cm³/mol. Clearly, the

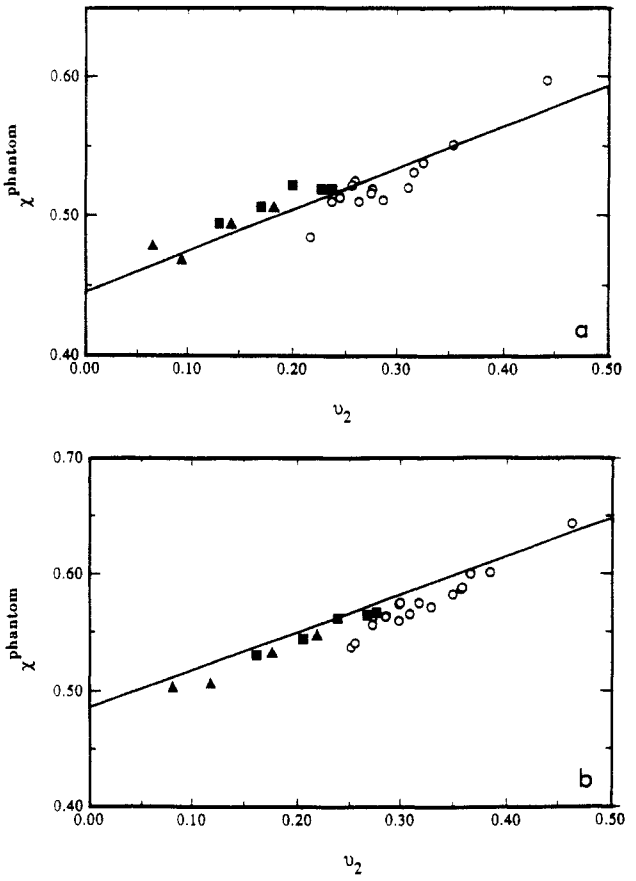

Figure 8. (a) χ as a function of υ_2 for the networks swollen in toluene. χ is calculated from the swelling results using the Flory–Rehner model with the phantom network assumption. The symbols are the same as in Figure 4. The line represents the interaction parameter obtained for solutions of un-cross-linked PDMS chains in toluene from ref 52. (b) Same as in (a) but for benzene. The line is from ref 55.

swelling and modulus data are correlated well by eq 13 over a wide range of equilibrium swelling extents ($0.06 < \upsilon_2$(toluene) < 0.44) and ($0.08 < \upsilon_2$(benzene) < 0.46) on the basis of the Flory–Rehner postulate and the phantom network model. Comparison of the experimental data with eq 12, based on the affine model, is almost as good as the results show in Figure 7 for the phantom model except for the data point related to the highest υ_2 and G_e/RT which lies in this case much further above the prediction than in Figure 7. This is due to the fact that eqs 12 and 13 differ only slightly in their left-hand sides. The difference is in general small because the additional $\upsilon_2/2$ term in eq 12 is small compared to the $\upsilon_2^{1/3}$ term for small υ_2's. For higher υ_2's the difference increases and over the wide range of modulus and swelling data examined here, the phantom model network gives clearly a better representation of the data.

Rather than using the literature value for χ, one can alternatively solve for χ in eq 13 and calculate its value as a function of υ_2. The resulting values of χ are reported in Figure 8a,b for toluene and benzene, respectively. In fact, linear regression applied to the data in Figure 8a for toluene, yields $\chi = 0.452 + 0.265\upsilon_2$, embarrassingly close to the literature value of linear PDMS chains in toluene[52] quoted earlier. In the case of benzene, the best fit line gives $\chi = 0.470 + 0.337\upsilon_2$. The values and the concentration dependencies of the calculated χ are reasonably close to the reported values for un-cross-linked PDMS solutions, which are represented by the lines in Figure 8a,b. Our results indicate that for the range in extent of swelling and cross-link density for this work, the Flory–Rehner model with the phantom network assumption describes the swelling data quite well. The sensitivity of the Flory–Rehner predictions to the value of χ is readily apparent from Figure 8. For the networks and solvents in this work, it does not appear necessary to introduce a cross-link density dependent interaction parameter[29] as the concentration dependence of χ observed here mimics fairly closely that of un-cross-linked chains.

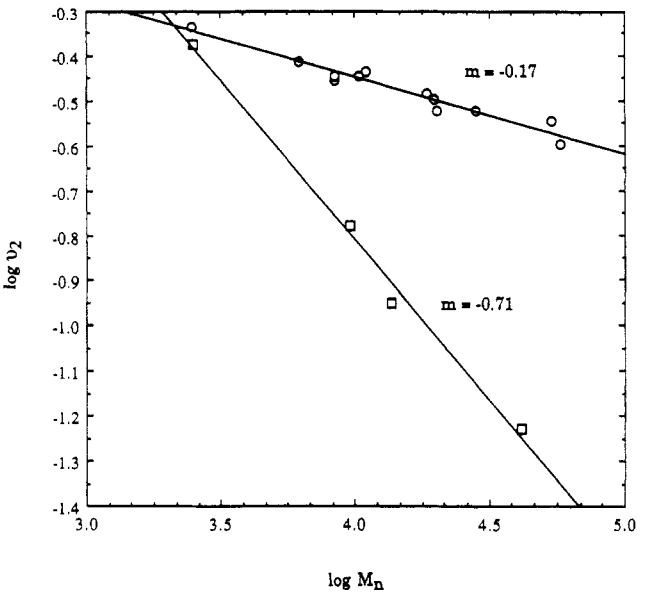

Figure 9. Scaling relationship between υ_2 and M_n for pure B_2 networks swollen in (○) our data; (□) data of ref 59. M_n is the number average molecular weight of the precursors used to prepare the networks.

As discussed in the Introduction, the c^* theorem predicts that υ_2 will scale with $(M_{n,el})^{-4/5}$. This scaling relationship assumes that the network chains can freely disintersperse upon swelling to equilibrium.[56] This assumption is not satisfied by melt end-linked model networks and we should not expect the c^* theorem to apply to our networks. We use the equilibrium swelling data in benzene for networks prepared from pure B_2 with very low soluble fractions (Table II), and approximate $M_{n,el}$ by M_{n,B_2}, to allow comparison with recently reported data discussed below. With this approximation, the scaling exponent between υ_2 and M_{n,B_2} in Figure 9 for our data (open circles) is −0.17. Although the range of M_{n,B_2} is small (slightly over a decade in magnitude), the scaling exponent obtained from Figure 9 is, as expected, considerably different than the c^* theorem prediction. The difference is due primarily to the large interspersion of chains that occurs in our swollen networks and that is not taken into account by the c^* theorem. We shall also see later that the approximation $M_{n,el} \approx M_{n,B_2}$ is too crude.

For the networks reported in Table II, it is easy to calculate the number of chains, n, in a volume of $(4/3)\pi \times (R_g(\text{melt}))^3$ of the dry network where R_g is the radius of gyration of the precursor B_2 chain. The value of n ranges from 1.9 to 10, as calculated using $R_{g,melt} = 0.23M^{0.51}$ obtained by Beltzung et al.[57] Upon swelling in toluene, the number of chains in a volume of $(4/3)\pi(R_g(\text{swollen network}))^3$ ranges from 1.7 to 8.7, as calculated using $R_g(\text{swollen network}) = 0.17M^{0.58}$ obtained by Beltzung et al.[58] Comparable small changes (~10%) in n from a dry network to its equilibrium swollen condition are expected for benzene. The changes in n upon swelling would still be of the same order if we assumed that in the swollen network the chain maintains its ideal random configuration. Thus, after swelling to equilibrium, the network

chains are still quite highly interspersed. The c^* theorem does not apply here because it depends upon the assumption of complete disinterspersion of chains upon swelling.

Our results are in contrast to the results recently reported by Oikawa and Murakami,[59,60] who examined end-linked PDMS networks swollen in benzene and reported very good agreement with the c^* theorem. Their results are also plotted in Figure 9, and an exponent of −0.71 is obtained, which is reasonably close to the c^* prediction of $-4/5$. There are several possible reasons for the discrepancy between the two sets of results. The soluble fractions reported by these workers are said to be "less than 5%". In comparison, the soluble fractions of the model networks in this work are typically less than 1%. Also, the equilibrium swelling extents in benzene are considerably greater in their work than the extents of swelling in this work, as shown in Figure 9. Finally, they noted that the molecular weights between cross-links calculated from the Flory–Rehner model were greater than the molecular weights of the precursors used to prepare the networks, which is the opposite of the results obtained in this work. These facts indicate that the networks prepared by these workers contain considerably more defects and that their networks are far from model networks. Thus, their assumption that $M_{n,el}$ equals M_{n,B_2} is a poor one. The proximity of their scaling exponent to $4/5$ appears, therefore, to be fortuitous.

A better approach to obtain $M_{n,el}$, incorporating the effect of entanglements and allowing us to include the data from our imperfect networks, is to equate $M_{n,el}$ to M_c, an effective molecular weight between cross-links obtained from the equilibrium elasticity measurements of the unswollen networks. For simplicity, we use the affine model and write

$$M_{n,el} = M_c = \rho_2 RT/G_e \qquad (14)$$

In words, this equation means that the number density of effective elastic strands is calculated according to the affine model from the experimental value of the modulus. The fact that we are using the affine model to calculate M_c instead of the phantom model, which is more appropriate, is unconsequential because in the phantom network, the right-hand side of eq 14 is multiplied by a factor $(1 - \mu/\nu)$ which is approximately constant for our networks and will not affect the correlation between log v_2 and log M_c that we are seeking. In Figure 10 we plot log v_2 versus log M_c for all the networks. The data could be fitted reasonably well with a straight line of slope −0.40. This is quite different from the scaling law prediction based on the c^* theorem ($-4/5$) but also quite different from the results of Flory–Rehner in the limit of $v_2 \ll 1$ which gives $v_2 \sim M_c^{-3/5}$. The latter result is obtained by expanding the logarithmic term of the Flory–Huggins expression and keeping up to the quadratic terms only. If, however, higher order terms in the expansion are kept, the Flory–Rehner expression with the phantom network assumption gives a very good agreement with the experimental results in Figure 10, where the curve is a representation of the Flory–Rehner equation with the logarithmic term expanded up to v_2^4 terms. One should note that the only adjustable parameter in the Flory–Rehner prediction is χ, which was determined independently in the literature. Figure 10 shows remarkably good agreement with the Flory–Rehner model, which assumes, on one hand, that excluded volume effects are negligible in the concentration range investigated (Flory–Huggins thermodynamics) and, on the other hand, that each effective elastic strand swells independently to equilibrium (equivalent to the c^* theorem).[61]

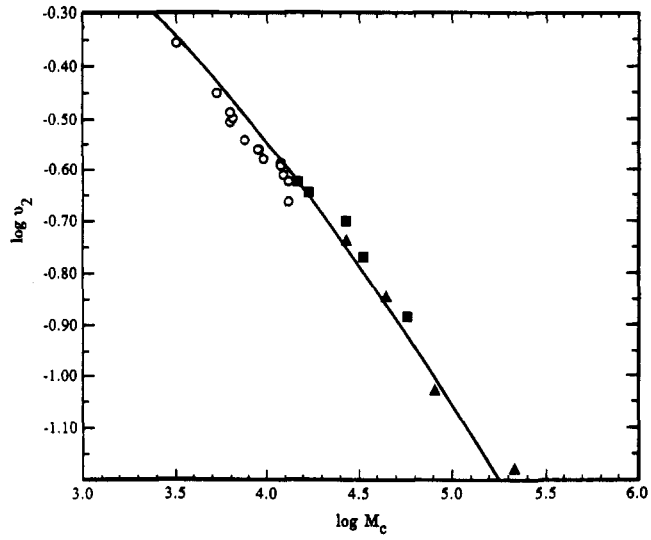

Figure 10. Scaling relationship between v_2 and M_c for the networks swollen in toluene. The symbols are the same as in Figure 4. The curve represents the Flory–Rehner predictions with the phantom network assumption and using the χ parameter from ref 52.

We show in the following paper that excluded volume effects are indeed negligible on the length scale of the hydrodynamic correlation length ($\xi_H \sim 100$ Å) as measured by dynamic light scattering.[62] We have no direct evidence on the second assumption concerning the stretching of effective elastic strands upon swelling, but our results indicate that because of topological constraints (entanglements), the original precursor chain may consist of several elastic strands leading to much smaller swelling than otherwise expected and as indicated in a recent theory by Panyukov.[61] On the length scale of a large precursor chain or of the hydrodynamic correlation length consisting of many effective elastic strands, swelling at the sublevel of an elastic strand is not inconsistent with negligible excluded volume effects on a longer length scale. It has been demonstrated that the size of a chain in the semidilute regime is larger than its ideal Gaussian size by only a factor of $v_2^{-1/8}$ and returns to its ideal size as v_2 is increased beyond the semidilute regime.[63]

Conclusions

The elastic behavior and equilibrium swelling of both model networks, prepared from difunctional (B_2) precursor chains, and imperfect networks, prepared from difunctional (B_2) and monofunctional (B_1) chain mixtures were studied. Average network parameters were calculated from the branching model developed by Macosko and Miller.[40-42] For the model networks, below a certain value of the calculated density of elastic chains (ν), the values of the equilibrium elastic modulus (G_e) appear to be constant and close to the plateau modulus of high molecular weight un-cross-linked PDMS, indicating that in this domain the major contribution to G_e arises from trapped entanglements. The behavior of the imperfect networks was quite different from that of the model networks. As ν was reduced by addition of B_1, the values of G_e dropped sharply from the plateau value. This is presumably because the architecture of these imperfect networks is considerably different from that of the model networks. Increasing the amount of B_1 in an imperfect network has a markedly different effect on the architecture of the network formed than increasing the molecular weight of B_2 in a model network. Both processes lead to a reduction in the resultant value of ν, but the former leads

to greater quantities of pendant chains and shorter elastic chains than the latter process. The experimental results indicate that imperfect networks are less effective at trapping entanglements than model networks of equivalent ν.

The swelling results are consistent with the mechanical measurements. For low values of ν, model networks appear to swell less than imperfect networks with the same value of ν. In agreement with the mechanical measurements, the presence of a greater amount of pendant material in the imperfect networks makes them less effective at trapping entanglements. The equilibrium swelling results are in good agreement with the postulate of a balance between the thermodynamic forces and the elastic forces if the actual measured modulus is used rather than the modulus determined from the branching model, which is underestimated because it neglects entanglements. In particular, we find that the Flory–Rehner model, coupled with the phantom network assumption, adequately predicts the experimental swelling results when the experimental value of the modulus is used.

Acknowledgment. We thank T. H. Mourey for molecular characterization of our precursor polymers. Part of the work presented here was performed in new laboratories in Olin Hall at Cornell University which were made possible by generous gifts from H. D. Doan and the Dow Chemical Co. Acknowledgment is also made to the donors of the Petroleum Research Fund, administered by the American Chemical Society, for partial support of this research.

Appendix

The expressions given below are easily obtained by following refs 40–42. The notation employed by Macosko and Miller will, for the most part, be used.

The weight fraction of soluble material is given by

$$w_{sol} = w_{A_4}\alpha^4 + w_{B_2}\beta^2 + w_{B_1}\beta \tag{A1}$$

where w_i is the weight fraction of species i in the initial reactant mixture, and α and β, which correspond to Macosko and Miller's $P(F_A^{OUT})$ and $P(F_B^{OUT})$, are probabilities of the occurrence of event F_A^{OUT} and F_B^{OUT}, respectively. F_A^{OUT} is defined as the event that if one picks up an A group at random and looks out away from the parent molecule, all paths are finite (none leads to an infinite network). F_B^{OUT} is defined is the same manner. One then finds that α and β are given by

$$\alpha = \left(\frac{4 - 3rp^2b_2}{4rp^2b_2}\right)^{1/2} - \frac{1}{2} \tag{A2}$$

$$\beta = rp\left[\left(\frac{4 - 3rp^2b_2}{4rp^2b_2}\right)^{1/2} - \frac{1}{2}\right]^3 + 1 - rp \tag{A3}$$

where r is the ratio of silane groups (A) to vinyl groups (B) in the reaction mixture, p is the extent of reaction of A groups, and b_2 is the mole fraction of the vinyl groups on the B_2 chains and is given by

$$b_2 = \frac{2B_2^\circ}{B_1^\circ + 2B_2^\circ} \tag{A4}$$

where B_1° and B_2° are the number of moles of species B_1 and B_2 in the reactant mixture. Equations A1–A4 are used to determine the extent of reaction p from w_{sol} since all other parameters are known from the composition of the initial reactant mixture.

The weight fraction of pendant and elastic material in the network, w_{pen} and w_{el}, respectively, and are given by

$$w_{pen} = 2w_{B_2}\beta(1-\beta) + w_{B_1}(1-\beta) + w_{A_4}\{4\alpha^3(1-\alpha) + 12\alpha^2(1-\alpha)^2M_A/M_{A_4} + 4\alpha(1-\alpha)^3M_A/M_{A_4}\} \tag{A5}$$

$$w_{el} = w_{B_2}(1-\beta)^2 + w_{A_4}\{(1-\alpha)^4 + 4(1 - M_A/M_{A_4}) \times (1-\alpha)^3\alpha + 6(1 - 2M_A/M_{A_4})(1-\alpha)^2\alpha^2\} \tag{A6}$$

where M_A is the molecular weight of one arm of an A_4 unit, and M_{A_4} is the molecular weight of A_4.

$M_{n,el}$, the number average molecular weight of the elastic chains, is given by

$$M_{n,el} = 2M_A + \frac{M_{n,B_2} + (M_{A_4} - 2M_A)C}{1 - C} \tag{A7}$$

where C is

$$C = \frac{3(1-\alpha)\alpha^2}{3(1-\alpha)\alpha^2 + 3(1-\alpha)^2\alpha + 3(1-\alpha)^3} \tag{A8}$$

and ν and μ are given by

$$\nu = \frac{A_4^\circ}{(1 - w_{sol})}[6\alpha(1-\alpha)^3 + 2(1-\alpha)^4] \tag{A9}$$

$$\mu = \frac{A_4^\circ}{(1 - w_{sol})}[4\alpha(1-\alpha)^3 + (1-\alpha)^4] \tag{A10}$$

References and Notes

(1) Flory, P. J. *Principles of Polymer Chemistry*; Cornell University Press: Ithaca, NY, 1953.
(2) James, H. M.; Guth, E. *J. Chem. Phys.* **1947**, *15*, 669.
(3) Flory, P. J. *J. Chem. Phys.* **1977**, *66*, 5720.
(4) Flory, P. J.; Erman, B. *Macromolecules* **1982**, *15*, 800.
(5) Mark, J. E.; Erman, B. *Rubberlike Elasticity: A Molecular Primer*; Wiley: New York, 1988.
(6) Langley, N. R. *Macromolecules* **1968**, *1*, 348.
(7) Dossin, L. M.; Graessley, W. W. *Macromolecules* **1979**, *12*, 123.
(8) Edwards, S. F.; Vilgis, T. A. *Rep. Prog. Phys.* **1988**, *51*, 243.
(9) Ball, R. C.; Doi, M.; Edwards, S. F.; Warner, M. *Polymer* **1981**, *22*, 1010.
(10) Edwards, S. F.; Vilgis, T. *Polymer* **1986**, *27*, 483.
(11) Flory, P. J.; Rehner, J. *J. Chem. Phys.* **1943**, *11*, 521.
(12) Herz, J.; Munch, J. P.; Candau, S. *J. Macromol. Sci.—Phys.* **1980**, *B18*, 267.
(13) Candau, S.; Peters, A.; Herz, J. *Polymer* **1981**, *22*, 1504.
(14) de Gennes, P. G. *Scaling Concepts in Polymer Physics*; Cornell University Press: Ithaca, NY, 1979.
(15) Mark, J. E. *Adv. Polym. Sci.* **1982**, *44*, 1.
(16) Erman, B.; Flory, P. J. *Macromolecules* **1982**, *15*, 806.
(17) Brotzman, R. W.; Flory, P. J. *Macromolecules* **1987**, *20*, 351.
(18) Mark, J. E.; Sullivan, J. L. *J. Chem. Phys.* **1977**, *66*, 1006.
(19) Soni, V. K.; Stein, R. S. *Macromolecules* **1990**, *23*, 5257.
(20) Valles, E. M.; Macosko, C. W. *Macromolecules* **1979**, *12*, 673.
(21) Macosko, C. W.; Benjamin, G. S. *Pure Appl. Chem.* **1981**, *53*, 1505.
(22) Gottlieb, M.; Macosko, C. W.; Benjamin, G. S.; Meyers, K. O.; Merrill, E. W. *Macromolecules* **1981**, *14*, 1039.
(23) Opperman, W.; Rennar, N. *Prog. Colloid Polym. Sci.* **1987**, *75*, 49.
(24) Gnanou, Y.; Hild, G.; Rempp, P. *Macromolecules* **1987**, *20*, 1662.
(25) Gerard, E.; Gnanou, Y.; Rempp, P. *Macromolecules* **1990**, *23*, 4299.
(26) Meyers, K. O.; Bye, M. L.; Merrill, E. W. *Macromolecules* **1980**, *13*, 1045.
(27) Neuburger, N. A.; Eichinger, B. E. *Macromolecules* **1988**, *21*, 3060.
(28) Gottlieb, M.; Gaylord, R. J. *Macromolecules* **1984**, *17*, 2024.
(29) McKenna, G. B.; Flynn, K. M.; Chen, Y. *Polym. Commun.* **1988**, *29*, 272.
(30) Bastide, J.; Picot, C.; Candau, S. *J. Polym. Sci.: Polym. Phys. Ed.* **1979**, *17*, 1441.

(31) Candau, S.; Bastide, J.; Delsanti, M. *Adv. Polym. Sci.* **1982**, *44*, 27.
(32) Andrady, A. L.; Llorente, M. A.; Sharaf, M. A.; Rahalkar, R. R.; Mark, J. E.; Sullivan, J. L.; Yu, C. U.; Falender, J. R. *J. Appl. Polym. Sci.* **1981**, *26*, 1829.
(33) Lee, C. L.; Frye, C. L.; Johannson, O. K. *Polym. Prepr., Am. Chem. Soc. Div. Polym. Chem.* **1969**, *10*, 1361.
(34) Lee, C. L.; Johannson, O. K. *J. Polym. Sci: Polym. Chem. Ed.* **1976**, *14*, 729.
(35) Lee, C. L.; Marko, O. W.; Johannson, O. K. *J. Polym. Sci.: Polym. Chem. Ed.* **1976**, *14*, 743.
(36) Lapp, A.; Herz, J.; Strazielle, C. *Makromol. Chem.* **1985**, *186*, 1919.
(37) Llorente, M. A.; Mark, J. E. *Macromolecules* **1980**, *13*, 681.
(38) Valles, E. M.; Macosko, C. W. *Macromolecules* **1979**, *12*, 521.
(39) Weiss, P.; Herz, J.; Rempp, P. *Makromol. Chem.* **1970**, *135*, 249.
(40) Macosko, C. W.; Miller, D. R. *Macromolecules* **1976**, *9*, 199.
(41) Miller, D. R.; Macosko, C. W. *Macromolecules* **1976**, *9*, 206.
(42) Miller, D. R.; Valles, E. M.; Macosko, C. W. *Polym. Eng. Sci.* **1979**, *19*, 272.
(43) He, X.; Lapp, A.; Herz, J. *Makromol. Chem.* **1988**, *189*, 1061.
(44) Venkataraman, S. K.; Coyne, L.; Chambon, F.; Gottlieb, M.; Winter, H. H. *Polym. Prepr., Am. Chem. Soc. Div. Polym. Chem.* **1988**, *29*, 571.
(45) Meyers, K. O. Ph.D. Thesis, Massachusetts Institute of Technology, 1980.
(46) Macosko, C. W.; Saam, J. C. *Polym. Bull.* **1987**, *18*, 463.
(47) Baselga, J.; Llorente, M. A.; Hernandez-Fuentes, I.; Pierola, I. F. *Eur. Polym. J.* **1989**, *25*, 477.
(48) Tobita, H.; Hamielec, A. E. *Polymer* **1990**, *31*, 1546.
(49) Patel, S. K. Ph.D. Thesis, Cornell University, 1991.
(50) Plazek, D. J.; Dannhauser, W.; Ferry, J. D. *J. Colloid Sci.* **1961**, *16*, 101.
(51) Ferry, J. D. *Viscoelastic Properties of Polymers*, 3rd ed.; Wiley: New York, 1980; p 360.
(52) Kuwahara, N.; Okazawa, T.; Kaneko, M. *J. Polym. Sci.: Part C* **1968**, 543.
(53) Patel, S. K.; Cohen, C. *Polym. Prepr., Am. Chem. Soc. Div. Polym. Chem.* **1990**, *31*, 124.
(54) Thirion, P.; Weil, T. *Polymer* **1984**, *25*, 609.
(55) Flory, P. J.; Shih, H. *Macromolecules* **1972**, *5*, 761.
(56) Daoud, M.; Bouchaud, E.; Jannink, G. *Macromolecules* **1986**, *19*, 1955.
(57) Beltzung, M.; Picot, C.; Rempp, P.; Herz, J. *Macromolecules* **1982**, *15*, 1594.
(58) Beltzung, M.; Herz, J.; Picot, C. *Macromolecules* **1983**, *16*, 580.
(59) Oikawa, H.; Murakami, K. *Rubber Chem. Technol.* **1987**, *60*, 579.
(60) Oikawa, H.; Murakami, K. *Macromolecules* **1991**, *24*, 1117.
(61) Panyukov, S. V. *JETP Lett. (Engl. Transl.)* **1990**, *51*, 253; *JETP* **1990**, *71*, 372.
(62) Patel, S. K.; Cohen, C. *Macromolecules*, following article in this issue.
(63) Daoud, M.; Cotton, J. P.; Farnoux, B.; Jannink, G.; Serma, G.; Benoit, H.; Duplessix, R.; Picot, C.; de Gennes, P.-G. *Macromolecules* **1975**, *8*, 804.

Registry No. Toluene, 71-43-2; benzene, 108-88-3.